Journal of Thermal Analysis and Calorimetry, Vol. 90 (2007) 2, 379–384

KINETIC ANALYSIS OF A THERMAL DECHLORINATION AND OXIDATION OF GADOLINIUM OXYCHLORIDE

H. C. Yang[1*], *Y. J. Cho*[1], *H. C. Eun*[2], *E. H. Kim*[1] *and I. T. Kim*[1]

[1]Nuclear Fuel Cycle R&D Group, Korea Atomic Energy Research Institute, P.O. Box 150 Yuseong, Daejeon 305-353, Korea
[2]Quantum Energy Chemical Engineering, University of Science and Technology, P.O. Box 52 Yuseong, Daejeon 305-333, Korea

Kinetics of a thermal dechlorination and oxidation of gadolinium oxychloride (GdOCl) originating from a molten salt process was investigated under various oxygen partial pressures by using a non-isothermal thermogravimetric (TG) analysis. The results of isoconversional analysis of the TG data suggests that the dechlorination and oxidation of GdOCl follows a single step reaction and the observed activation energy was determined as 137.7±4.1 kJ mol^{-1}. The kinetic rate equation was derived for a conversion of the GdOCl with a linear-contacting boundary reaction model. The power dependency for oxygen and the pre-exponential factor was determined as 0.306 and 1.012 s^{-1} Pa$^{-0.306}$, respectively.

Keywords: *gadolinium oxychloride, linear-contacting boundary reaction model, non-isothermal thermogravimetric analysis, oxidation, thermal dechlorination*

Introduction

Rare earth metals and alloys are widely used in different fields of modern technology [1–3]. An electrochemical separation and an electrochemical synthesis in molten chloride salts are promising technologies for obtaining pure RE metals, RE oxides and RE alloys [4]. By-products of these electrochemical processes include RE oxychlorides such GdOCl, NdOCl and SmOCl, etc. Pure RE oxides are additionally obtained by a heating of the RE oxychlorides to emit gaseous chlorines in the presence of oxygen as:

$$2REOCl+1/2O_2(g)=RE_2O_3+Cl_2(g)$$

Detailed kinetics of the above dechlorination and oxidation reaction of REOCl have not been reported in the existing literatures.

TG methods, such as isothermal and non-isothermal methods have been used widely to establish the kinetics for a conversion of many solids [5–9]. A non-isothermal TG study has an advantage in that a wide range of temperatures are covered with a single experiment [10]. This study investigated the dechlorination and oxidation behavior of a typical rare earth oxichloride, gadolinium oxychloride (GdOCl) by using a non-isothermal TG method. The objectives of this study are to establish a detailed kinetic model and the kinetic parameters of the dechlorination and oxidation reaction of GdOCl under high-temperature oxidizing atmospheres.

Theoretical

The conversion of GdOCl into Gd_2O_3 in the presence of oxygen can be described by the following reaction scheme:

$$2GdOCl+1/2O_2(g)\rightarrow Gd_2O_3+Cl_2(g)$$

The influence of the temperature and that of an oxygen partial pressure on the above reaction can be described with an Arrhenius equation and a power law approach, respectively. The reaction rate of the above reaction is thus described as:

$$\frac{d\alpha}{dt} = k_0 (P_{O_2})^n \exp\left(-\frac{E}{RT}\right) f(\alpha) \qquad (1)$$

where α is the extent of a conversion, k_0 the reaction rate constant (s^{-1} Pa^{-n}), P_{O_2} the oxygen partial pressure (Pa) and n the power dependency of the oxygen partial pressure. The function $f(\alpha)$ represents the influence of a conversion on the conversion rate. In the case of a non-isothermal reaction, the applied heating rates are constant and the temperature can be expressed as $T=Bt+T_0$ in which the constant heating rate, B, is given as $dT/dt=B$. Using this transformation of Eq. (1) and a separation of the variables results in:

$$\frac{d\alpha}{f(\alpha)} = \frac{k_0}{B} (P_{O_2})^n \exp\left(-\frac{E}{RT}\right) dT \qquad (2)$$

which can be rewritten as:

* Author for correspondence: nhcyang@kaeri.re.kr

1388–6150/$20.00

Akadémiai Kiadó, Budapest, Hungary
Springer, Dordrecht, The Netherlands

$$g(\alpha) = \frac{ZE}{BR} p(y) \quad (3)$$

in which $g(\alpha)$ is the result of an integral on the left hand side of Eq. (2), $Z = k_0(P_{O_2})^n$ and $p(y)$ is a function of the temperature integral on the right hand side of Eq. (2):

$$p(y) = \int_{y_0}^{y_c} \frac{e^{-y}}{y^2} dy = \frac{e^{-y}}{y^2} + \int_{y_0}^{y_c} \frac{e^{-y}}{y} dy \quad (4)$$

in which $y=-E/RT$. The kinetic parameters Z and E in Eq. (3) are invariable for a single step reaction. By using a reference at a half conversion (α=0.5), Eq. (3) is converted into

$$\alpha(0.5) = \frac{ZE}{BR} p(y_{0.5}) \quad (5)$$

where $y_{0.5}=E/RT_{0.5}$. Dividing Eq. (3) by Eq. (5), the following equation is given

$$\frac{g(\alpha)}{g(0.5)} = \frac{p(y)}{p(y_{0.5})} \quad (6)$$

Theoretical master plots are given by plotting $g(\alpha)/g(0.5)$ for various $g(\alpha)$ functions. In order to obtain experimental master plots of $p(y)/p(y_{0.5})$ *vs*. a conversion α from the experimental data, the temperature as a function of α and E should be established in advance. Equation (4) is not analytically soluble and many approximations have been proposed and they are still being discussed [11–13]. An accurate approximate formula for $p(y)$ proposed by Wanjun *et al*. [14] is applied in the present study.

$$-\ln[p(y)] = 0.377739 + 1.894661 \ln y + 1.001450 y \quad (7)$$

By introducing Eq. (7) into Eq. (3), Eq. (8) is obtained.

$$\ln(B/T^{1.894661}) = \ln[ZE/Rg(\alpha)] + 3.635041 - 1.894661 \ln E - 1.001450(E/RT) \quad (8)$$

Assuming that the reaction model, $g(\alpha)$, does not change for all the conversion levels under a constant oxygen partial pressure, a plot of $\ln(B/T^{1.894661})$ *vs*.the reciprocal of an absolute temperature ($1/T$) should have the same slopes as Eq. (8), which provide the activation energy of the reaction as:

$$E = -\frac{R}{1.001450}\left[\frac{d\ln(B/T^{1.894661})}{d(1/T)}\right] \quad (9)$$

Once the activation energies have been determined, an appropriate kinetic model can be found by a comparison of the experimental master plots with the theoretical master plots for various reaction models. Based on the determined activation energy E and conversion model $g(\alpha)$, the Z values, which are different for each oxygen partial pressure, are determined by the logarithms of Eq. (3).

$$\ln[p(y)] = \ln B - \ln(ZE/R) + \ln[g(\alpha)] \quad (10)$$

The reaction order with respect to the oxygen partial pressure, n, is estimated from the slope of a graph for the logarithmic of Z *vs*. the logarithmic of the oxygen partial pressure (P_{O_2}).

$$\ln Z = \ln k_0 + n \ln P_{O_2} \quad (11)$$

Experimental

Materials and methods

Synthesis and analysis of GdOCl and its post-TG product

Powdered gadolinium oxychloride (GdOCl) was synthesized in LiCl–KCl molten salt. The experimental apparatus for synthesizing the GdOCl is shown in Fig. 1. The experimental apparatus consists of an alumina crucible with an inner of 65 mm, an external electric heating ceramic furnace system and an oxygen supplying unit. Anhydrous $GdCl_3$ with a purity of 99.99% was premixed with a LiCl–KCl solid salt with a purity of 99.9% (LiCl: 44.2 mass%, eutectic point: 633 K) in an alumina crucible. The crucible containing the mixture was heated up to 723 K in a stainless-steel column and oxygen was sparged from the bottom. After a 5-h oxygen sparging, the mixture of the precipitate was sampled and dissolved in distilled water. A pure sample powder of GdOCl, was then obtained by a vacuum filtration. SEM photographs of the obtained GdOCl powder and its post-TG product, Gd_2O_3 powder, are shown in Fig. 2. Speciation of the obtained pre- and post-TG samples were performed by a powdered XRD pattern analysis and the results are shown in Fig. 3.

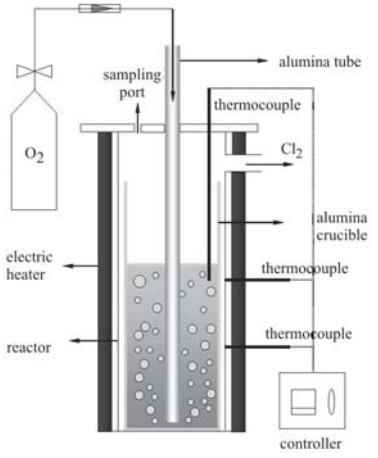

Fig. 1 A schematic experimental apparatus for synthesizing the GdOCl

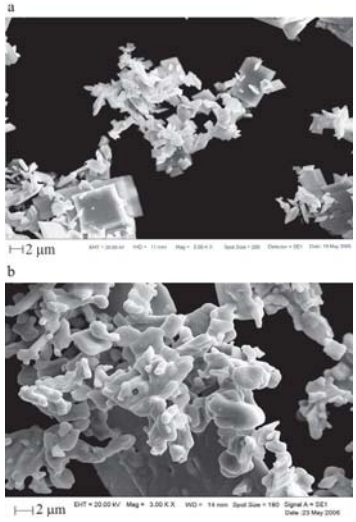

Fig. 2 SEM photograph of a – GdOCl, b – Gd_2O_3

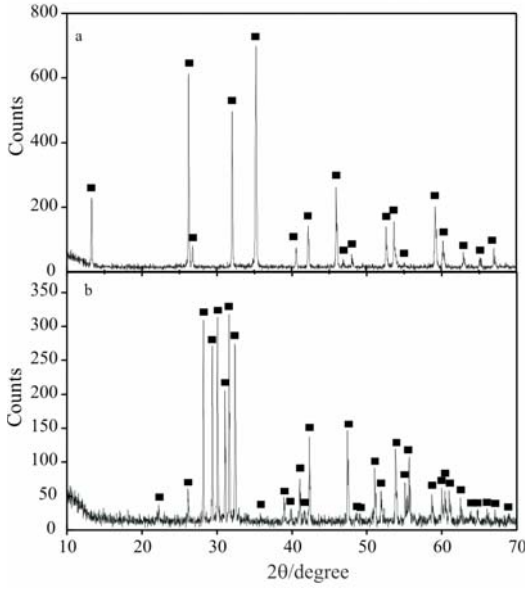

Fig. 3 Powdered XRD patterns of a – synthesized GdOCl and b – its post-TG product, Gd_2O_3

TG analysis

Non-isothermal TG analyses by using TG/DTA (SDT-6120, TA Instruments Inc.) were performed from room temperature to 1673 K. The temperature of the furnace was programmed to rise from room temperature to 1073 K with a heating rate of 50 K min^{-1}. After an initial rapid heating, the furnace was slowly heated from 1073 to 1473 K with heating rates of 5, 10, 15 and 20 K min^{-1}. At each heating rate condition, four oxygen partial pressures were tested: 21, 50, 75 and 100% of oxygen and the remainder consisted of pure nitrogen (>99.9%).

Results and discussion

Mass change patterns of the GdOCl

The mass loss as a function of temperature of the GdOCl powders at different heating rates under a fixed O_2 condition and those at a fixed heating rate under different O_2 conditions are plotted in Figs 4 and 5, respectively. Increasing the heating rate or decreasing the gaseous oxygen concentration resulted in a decrease in the conversion rate. This indicates that the conversion of GdOCl into Gd_2O_3 is an oxygen-dependent endothermic reaction.

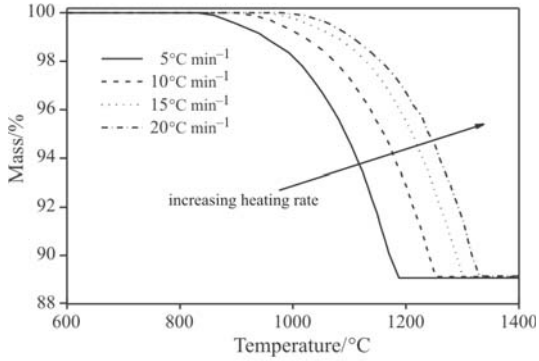

Fig. 4 Typical mass loss patterns of GdOCl at various heating rates under a fixed oxygen partial pressure (50% oxygen)

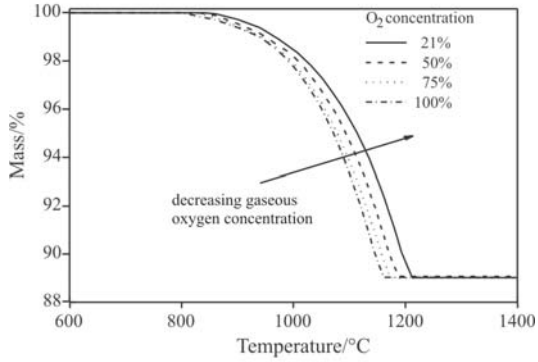

Fig. 5 Typical mass loss patterns of GdOCl at a fixed heating rate (5°C min^{-1}) under various O_2 partial pressures

Activation energy estimation

Obtained thermo-gravimetric data was analyzed to determine the activation energy for different levels of a conversion by using Eq. (9). A typical plot constructed to evaluate the slopes $d\ln(B/T^{1.894661})/d(1/T)$ is shown in Fig. 6. If the conversion mechanisms were the same at all the conversion levels, the lines would all have the same slopes, which is the case here. This process was repeated for different sets of experiments at different partial pressures of oxygen. Determined activation energies for all the different conditions are plotted in Fig. 7. It was observed from Fig. 7 that the

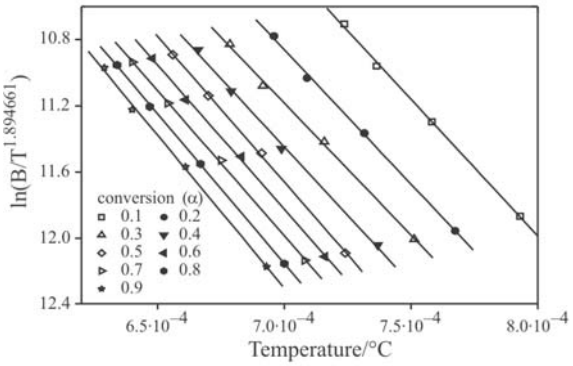

Fig. 6 Typical isoconversional plots for the determination of an activation energy of the dechlorination and oxidation of GdOCl (50% oxygen)

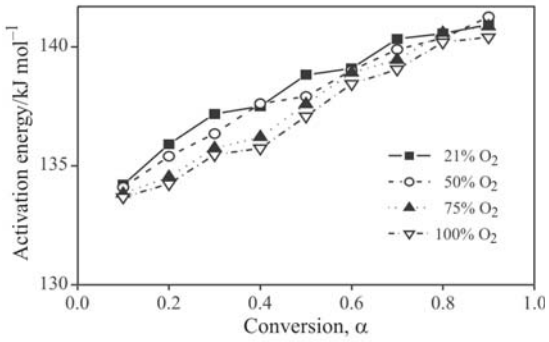

Fig. 7 Determined activation energy of the dechlorination and oxidation of GdOCl under different oxygen partial pressures, as a function of conversion

activation energy is continuously increasing but it is a weak function of a conversion. This suggests that the dechlorination and oxidation of GdOCl follows a single step reaction. A slow but steady increase in the activation energy as a weak function of the conversion can probably be explained by the interference of Gd_2O_3 at the reaction interface, which increases as the reaction proceeds. The activation energy were determined as 137.7±4.1 kJ mol^{-1}. It should be noted that these results were obtained without a knowledge of the reaction model $f(\alpha)$.

Kinetic model determination

Following the evaluation of the activation energy, the conversion model was determined by means of master-plots methods. By using the determined value of the activation energy E as a function of α for all the different conditions, the experimental master plots were constructed as shown in Fig. 8. The theoretical master plots of the various kinetic functions listed in Table 1 are also plotted as solid lines in Fig. 8. The comparison of the experimental master plots with the theoretical ones indicates that the mechanisms of the conversion of GdOCl into Gd_2O_3 could probably be

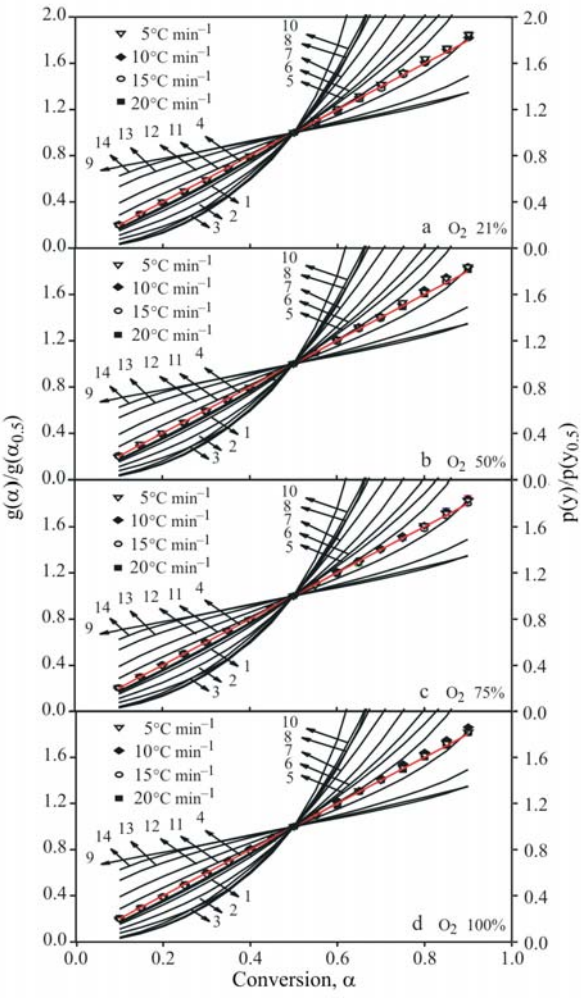

Fig. 8 Master plots of theoretical $g(\alpha)/g(\alpha_{0.5})$ *vs.* α for various reaction models (solid lines, as enumerated in Table 1) and experimental values of $p(y)/p(0.5)$ for different O_2 conditions (symbols)

described by the linear-contacting phase boundary reaction [$g(\alpha)=\alpha$]. Therefore the corresponding model equation describing the conversion of GdOCl into Gd_2O_3 is given by:

$$g(\alpha) = \alpha = k_0 \exp\left(-\frac{E}{RT}\right)(P_{O_2})^n t \qquad (12)$$

Evaluation of the oxygen power dependency and pre-exponential factor

By introducing the determined reaction model, $g(\alpha)=\alpha$, into Eq. (3), Eq. (13) is obtained.

$$\alpha = \frac{ZE}{BR} = p(y) \qquad (13)$$

The plots of α *vs.* $p(y)$ for all the different conditions were constructed in Fig. 9. By using Eq. (13), the Z values were determined from the slopes of the fitted lines (ZE/BR) shown in Fig. 9. From the aver-

Table 1 Kinetic model equations examined in this study

No.	Model	$f(\alpha)$	$g(\alpha)$
Reaction order (n)		$(1-\alpha)^n$	
1	1st order		$-\ln(1-\alpha)$
2	2nd order		$(1-\alpha)^{-1}-1$
3	3rd order		$1/2[(1-\alpha)^{-2}-1]$
Phase boundary reaction			
4	One-dimensional symmetry	1	α
5	Cylindrical symmetry	$2(1-\alpha)^{0.5}$	$1-(1-\alpha)^{0.5}$
6	Spherical symmetry	$3(1-\alpha)^{2/3}$	$1-(1-\alpha)^{1/3}$
Diffusional			
7	One-dimensional	$1/2\alpha$	α^2
8	Two-dimensional	$[-\ln(1-\alpha)]^{-1}$	$(1-\alpha)[\ln(1-\alpha)]+\alpha$
Three-dimensional spherical symmetry			
9	Jander equation	$1.5(1-\alpha)^{2/3}[1-(1-\alpha)^{1/3}]^{-1}$	$[1-(1-\alpha)^{1/3}]^2$
10	Guinstling–Brounshtein	$1.5[(1-\alpha)^{1/3}-1]^{-1}$	$(1-2\alpha/3)-(1-\alpha)^{2/3}$
Nuclei-growth			
11	Avrami–Erofeev (n=1.5)	$1.5(1-\alpha)[-\ln(1-\alpha)]^{1/3}$	$[-\ln(1-\alpha)]^{2/3}$
12	Avrami–Erofeev (n=2)	$2(1-\alpha)[-\ln(1-\alpha)]^{1/2}$	$[-\ln(1-\alpha)]^{1/2}$
13	Avrami–Erofeev (n=3)	$3(1-\alpha)[-\ln(1-\alpha)]^{2/3}$	$[-\ln(1-\alpha)]^{1/3}$
14	Avrami–Erofeev (n=4)	$4(1-\alpha)[-\ln(1-\alpha)]^{3/4}$	$[-\ln(1-\alpha)]^{1/4}$

Table 2 Determined kinetic parameters of the conversion of GdOCl into Gd_2O_3

Reaction model	Activation energy, E/kJ mol^{-1}	Pre-exponential factor, k_0/s^{-1} Pa$^{-0.306}$	Power dependence of oxygen, n
$g(\alpha)=\alpha$	137.7±4.1	1.012	0.306

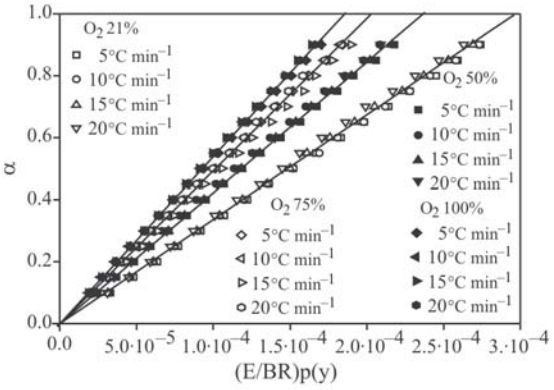

Fig. 9 Determination of Z values by plotting α *vs.* $(E/BR)p(y)$ for different O_2 conditions

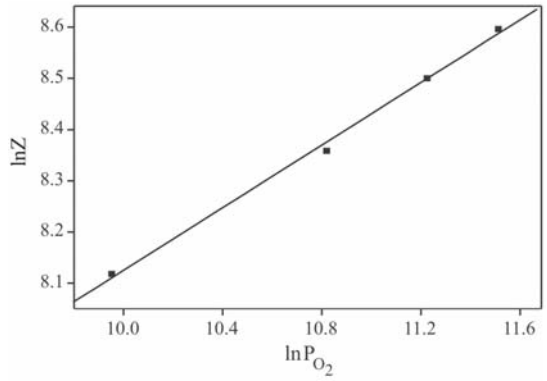

Fig. 10 Determination of pre-exponential factor A and oxygen power dependency n from the slopes of the plots ln$Z$ *vs.* $\ln P_{O_2}$

aged Z values for the corresponding oxygen partial pressures, the plots of ln$Z$ *vs.* $\ln P_{O_2}$ were constructed and the results are shown in Fig. 10. The oxygen power dependency n and the pre-exponential factor k_0 were determined by using Eq. (11) and the slope and the intercept of the linearly fitted line in Fig. 10. The slope (n) and the intercept (lnk_0) of the fitted line were determined as 0.3057 and 0.01244, respectively. Finally, parameters of the kinetic model Eq. (12) were determined as listed in Table 2.

Conclusions

The mechanisms of the dechlorination and oxidation of GdOCl powder originating from a molten salt process could be established by non-isothermal TG analyses under various oxygen partial pressures. The conversion of GdOCl into Gd_2O_3 at high temperatures appeared to be an oxygen-dependent endothermic and one-step reaction. The observed activation energy of the reaction was determined as 137.7±4.1 kJ mol^{-1}.

Kinetic rate equation was derived for the conversion of GdOCl powder with a linear-contacting boundary reaction model, which might be attributed to the characteristics of the plate crystal geometry of the GdOCl powder. The power dependency for oxygen was determined as 0.306 and the pre-exponential factor was determined as 1.012 s^{-1} $Pa^{-0.306}$.

Acknowledgements

This study has been carried out under the Nuclear R&D Program by the Korean Ministry of Science and Technology.

References

1 H. Konishi, T. Nohira and Y. Ito, Electrochim. Acta, 48 (2003) 563.
2 H. Konishi, T. Nishikiori, T. Nohira and Y. Ito, Electrochim. Acta, 48 (2003) 1403.
3 S. A. Kuznetsov and M. Gaune-Escard, Electrochim. Acta, 46 (2001) 1101.
4 Y. Yamamura, I. Wu, H. Zhu, M. Endo, N. Asao, M. Mohamend and Y. Sato, Molten Salt Chem. Technol., 5 (1998) 355.
5 M. Ginic-Markovic, N. R. Choudhury, J. G. Matisons and D. R. G. Williams, J. Therm. Anal. Cal., 59 (2006) 409.
6 N. Shamara, A. K. Sood, S. S. Bhatt and S. C. Chaudhry, J. Therm. Anal. Cal., 61 (2000) 779.
7 B. Saha, A. K. Maiti and A. K. Ghoshal, Thermochim. Acta, 444 (2006) 46.
8 M. A. Gabal, Thermochim. Acta, 412 (2006) 55.
9 B. Rodut, Ch. Borgeat, B. Berger, P. Folly, B. Alonso, J. N. Aebisher and F. Stoessel, J. Therm. Anal. Cal., 80 (2005) 229.
10 N. Mehta and A. Kumar, J. Therm. Anal. Cal., 83 (2006) 401.
11 C. D. Doyle, J. Appl. Polym. Sci., 4 (1962) 639.
12 R. C. Everon, H. W. J. P. Neomagus and D. Njapha, Fuel, 85 (2006) 418.
13 E. Sima-Ella, G. Yuan and T. Mays, Fuel, 84 (2005) 1920.
14 T. Wanjun, L. Yuwen, Z. Hen,W. Zhiyong and W. Cunxin, J. Therm. Anal. Cal., 74 (2003) 309.

Received: September 1, 2006
Accepted: January 31, 2007
OnlineFirst: June 1, 2007

DOI: 10.1007/s10973-006-7947-x